COMP3022 INFORMATION VISUALISATION PROJECT

KAIYI CHEN - 20318199, GIOVANNI BUABENG – 20345673, PARSA BAHRAMI – 20364490

1 INTRODUCTION

In April 2019, St. Himark, a vibrant city of nearly a quarter million people located by the Oceanus Sea, experienced a devastating earthquake that severely compromised its infrastructure and overwhelmed emergency services. In response, city officials and emergency responders utilized every available resource, including a newly launched damage reporting app, to assess the damage and prioritize aid distribution effectively. This app enabled the community to provide real-time updates, enhancing the accuracy of the data collected on the earthquake's impact.

This project leverages visual analytics to analyze seismic data, citizen reports, and the geographic context of St. Himark to refine emergency response strategies. By examining data from before and after the quake, our aim is to pinpoint critical areas, assess the reliability of reports, and understand the city's evolving conditions post-disaster. Our analysis seeks to offer insights that optimize resource allocation and improve emergency responses, ensuring aid is directed to where it is most needed.

2 RELATED WORK

Technological advancements have revolutionized disaster management by democratizing information access and enhancing situational awareness through tools like mobile apps, social media, and crisis-mapping systems. These systems integrate real-time data from affected populations, enabling quick, informed responses but face challenges in scalability and internet dependency. The crisis-mapping system developed by Avvenuti et al. (2016) leverages Twitter data for real-time damage visualization, proven effective in Italian disasters with a high validation score, though its utility is limited in areas with poor connectivity.

Future enhancements could introduce offline capabilities and improved privacy measures, boosting user trust and system resilience. Additionally, the system by Ishida and Ohyanagi (2020) integrates diverse data sources to adapt dynamically to real-time information, enhancing emergency management but needing broader testing for scalability and generalizability.

These tools have significantly improved response times and outcomes by enabling advanced data analysis through visual analytics. For instance, the flood decision support dashboard by Saha et al. (2018) integrated multiple data sources to enhance flood risk forecasting, demonstrating the powerful combination of community engagement and analytics. Similarly, research by Wang, Lee, and Lee (2020) showed that visual analytics could reduce emergency response times by 30%, crucial for effective evacuation and resource distribution.

Despite their benefits, these systems require accurate, real-time data and need to be user-friendly to be effective across different disaster scenarios. Future advancements should focus on improving data integration and interface design, with potential developments in artificial intelligence to enhance predictive analytics, thus strengthening disaster management and community resilience. These improvements are critical for ensuring that disaster management tools remain effective and adaptable to evolving challenges.

3 METHODS / DESIGN

The challenge presented by the St. Himark earthquake incident demanded a robust visual analytics approach to aid emergency responders in their decision-making process. Our methodology had to address three key objectives: prioritizing neighborhoods for response, assessing the reliability of reports, and monitoring changes over time. To achieve this, we employed a combination of data transformation, statistical analysis, and interactive visualization techniques using various Python libraries including Matplotlib, Seaborn, Altair, NumPy, NetworkX, and Plotly.

The foundational concepts in the visualization and analysis system described by Ishida and Ohyanagi (2020) were adapted for this project to systematically illustrate the process of creating visual representations from source data to final views. This visualization pipeline effectively transitions data through various stages. Specifically tailored to this project's needs, the adapted pipeline accommodates the unique requirements of domain-specific data, facilitating the development of user interactive visualizations that enable a deeper understanding and more refined visual displays.

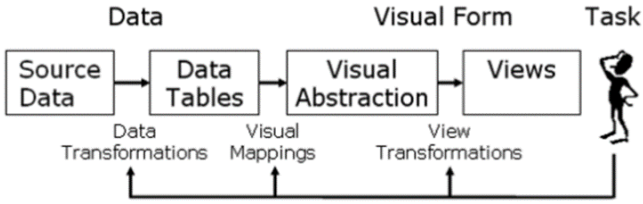

Figure 1- Flowchart illustrating the visualization design pipeline.

In our analysis of earthquake damage in St. Himark, we leveraged Python's robust data manipulation capabilities to effectively manage and analyze data from CSV files. These files, loaded through Google Colab's drive mount feature, included comprehensive post-earthquake damage reports.

We standardized all timestamps to ensure consistency across entries and filled missing data with the mean values of respective columns to maintain data integrity. Categorical damage descriptions were also converted into numerical scales to facilitate quantitative analysis. We employed Pandas functions such as groupby, reset_index, and melt to restructure and aggregate data, setting a strong foundation for detailed analysis.

We utilized Seaborn and Matplotlib to create heatmaps that illustrate infrastructure damage across neighborhoods, employing customized color maps for enhanced clarity. Altair supported our development of interactive time series visualizations, allowing users to focus on specific locations or periods. This adaptability enabled the provision of customized insights crucial for disaster response efforts.

We further enhanced our analysis by generating correlation matrices with Seaborn to identify relationships between different types of infrastructure damage. Additionally, Altair and Plotly Express were used to produce dynamic, interactive visualizations, such as line charts and scatter plots, facilitating an engaging data exploration experience.

NetworkX played a critical role in mapping out the interconnections between key nodes like neighborhoods and hospitals, crucial for pinpointing critical areas that influence wider response and recovery strategies. To ensure our visualizations were interactive and

responsive, we integrated D3.js for advanced data binding to SVG elements, enabling real-time updates and interactions.

The interface was designed with a focus on ease of use and accessibility, incorporating interactive elements like sliders, dropdowns, and buttons to adapt to user needs. The responsive design ensured that users received immediate feedback, which is vital for effective decision-making during emergency management.

Drawing upon the proven effectiveness of integrated GIS and mobile applications in disaster management scenarios, as demonstrated by Sharma et al. in the aftermath of cyclone Gaja, we aligned our strategies to utilize similar technological advantages (Sharma et al., 2020). In their study, GIS-enabled mobile applications significantly enhanced the speed and efficiency of disaster response by facilitating improved communication and resource allocation among emergency responders. This precedent validates our use of advanced data visualization tools like Seaborn, Altair, and D3.js, underscoring our commitment to adopting best practices in disaster data analysis and management.

By employing these technologies, we not only follow in the footsteps of successful prior implementations but also push the boundaries by integrating interactive and network visualization tools to better understand and respond to the complex dynamics of disaster impacts. This strategic incorporation of technology ensures that our analysis remains robust, responsive, and fundamentally geared toward enhancing disaster preparedness and response capabilities in urban settings.

The flowchart outlines our systematic approach to managing and visualizing earthquake damage data. We begin by importing data from a CSV file into a pandas DataFrame, setting the stage for robust data analysis. This involves converting 'time' entries into datetime objects for precise time-series analysis and indexing and grouping the data by hour and location to enable detailed examination.

In the statistical analysis phase, we calculate the mean and standard deviation for each data group, forming the basis for plotting error bars that highlight data variability and potential outliers.

Our workflow also enhances interactivity by mapping location IDs to neighborhood names and integrating interactive dropdown selectors, allowing users to dynamically explore and manipulate the data according to their investigative needs.

During the visualization execution, we define functions for plotting time series with error bars to illustrate data variability clearly. We incorporate interactive features like customized hover templates and optimize the plot layout for an effective presentation, making the data exploration process both informative and user-friendly.

The final interactive display of the plot allows users to actively engage with and derive insights from the visualized data, enhancing their understanding and aiding the decision-making process. This clear, accessible, and manipulatable visualization underscores our commitment to rigorous methodological practices and transparency, ensuring stakeholders can effectively interact with and benefit from the analyzed data.

This flowchart validates our commitment to methodological rigor and transparency, ensuring that stakeholders can easily understand and replicate our analytical process. To further substantiate our approach, we refer to Ishida & Ohyanagi, who implemented a visualization and analysis system for historical disaster records, highlighting the effectiveness of integrating advanced data processing and interactive visualization tools in comprehending complex datasets (Ishida and Ohyangi, 2020)

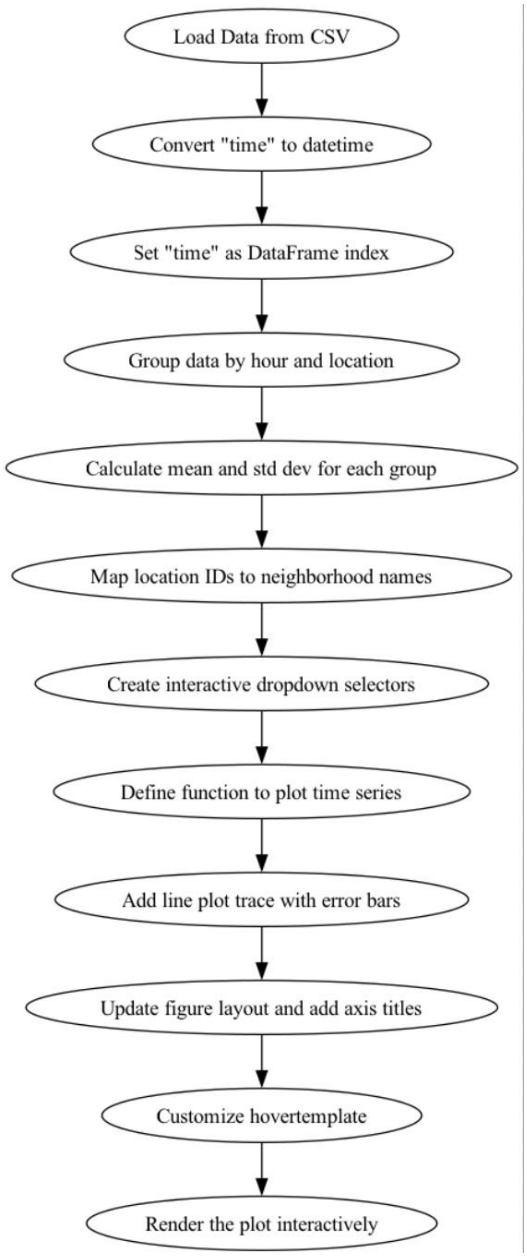

Figure 2 - Flowchart for the time series graph generation process.

4 IMPLEMENTATION

Implementation Overview:

For Analysis Task 1, our implementation focused on applying visual analytics techniques to prioritize emergency response efforts by identifying the hardest-hit neighborhoods. This section describes the specific tools, technologies, and processes used to implement the visualizations and analyses discussed in the "Methods/Design" section.

4.1 Data Loading and Cleaning

Python and Pandas: We utilized Python's Pandas library to load and preprocess the data. Initial steps involved cleaning the data by removing duplicates and correcting erroneous entries.

```
import pandas as pd
```

Figure 3 – Code for importing Python Pandas library.

```
[52] data = pd.read_csv('/content/drive/MyDrive/InfoViz/mc1-reports-data-cleaned (1).csv')
```

Figure 4 – Code for loading the data.

Timestamp Standardization:

We standardized timestamps to ensure consistency across the dataset, crucial for time series analysis.

```
data['time'] = pd.to_datetime(data['time'], dayfirst=True)
```

Figure 5 - Code for the standardization of time column.

4.2 Analytical Techniques and Visualization Implementation

Severity Index Calculation:

We computed a severity index for each neighborhood by averaging the damage ratings across all reports. This index served as a quantitative measure of overall damage severity.

```
data['infrastructure_damage'] = data[['sewer_and_water', 'power', 'roads_and_bridges']].mean(axis=1)
damage_by_neighborhood = data.groupby('location')['infrastructure_damage'].mean().reset_index()
damage_by_neighborhood_sorted = damage_by_neighborhood.sort_values(by='infrastructure_damage', ascending=False)
```

Figure 6 - Code for the calculation of the severity.

Temporal Analysis:

For dynamic and static visualizations, respectively, we employed Plotly and Matplotlib to create temporal graphs that display how damage reports evolved over time.

Heatmap of Infrastructure Damage:

Using Seaborn, a heatmap was generated to visually represent the infrastructure damage across neighborhoods, aiding in quick identification of severely affected areas:

```
import numpy as np
import seaborn as sns
import matplotlib.pyplot as plt


# This matrix will have a single value per row, representing the infrastructure damage
data_matrix = damage_by_neighborhood_sorted[['infrastructure_damage']].values

# Creating a figure and axis for the plot
plt.figure(figsize=(10, 10))

# Creating a heatmaps
sns.heatmap(data_matrix, annot=True, fmt=".2f", cmap="viridis", yticklabels=damage_by_neighborhood_sorted['location'].astype(str))

# Adding labels and title for clarity
plt.title("Infrastructure Damage by Neighborhood")
plt.ylabel("Neighborhood ID")
plt.xlabel("Infrastructure Damage Rating")

# Adjusting the y-axis for better visibility
plt.yticks(rotation=0)

plt.show()
```

Figure 7 - Code for the heatmap.

Interactive Scatter Plot of Impact vs. Vulnerability:

Developed using Plotly, this interactive plot allowed users to explore the relationship between the impact of the damage and the vulnerability of neighborhoods, aiding in resource allocation decisions.

```
# Create the scatter plot
fig = px.scatter(agg_reports, x="impact", y="vulnerability",
                 size="population", color="neighborhood",
                 hover_name="neighborhood", size_max=60,
                 title="Impact vs. Vulnerability Across Neighborhoods")

fig.show()
```

Figure 8 - Code for the Scatter Plot

Correlation Analysis of Damage Factors:

A correlation matrix was utilized to understand the relationships between various damage factors, providing insights into how different types of damage were interrelated.

```
# Assuming `data` includes the relevant columns
correlation_matrix = data[['sewer_and_water', 'power', 'roads_and_bridges', 'medical', 'buildings']].corr()

# Plotting using seaborn for a refined implementation
plt.figure(figsize=(10, 8))

# Create a heatmap with additional options for better visualization
sns.heatmap(correlation_matrix, annot=True, cmap='coolwarm', center=0,
            linewidths=.5, cbar_kws={"shrink": .5}, square=True)

# Enhancements for readability
plt.title('Correlation Matrix of Infrastructure Damage Reports', fontsize=16)
plt.xticks(rotation=45, ha='right', fontsize=12)
plt.yticks(fontsize=12)

# Tight layout often provides a better visual arrangement
plt.tight_layout()

plt.show()
```

Figure 9 - Code for the Correlation Plot.

4.3 Implementation of St. Himark Map

Data Integration and Processing

Data handling was executed through D3.js, loading and preprocessing data from mc1-reports-data-cleaned.csv. This included cleaning duplicates, normalizing data formats, and transforming categorical damage assessments into numerical values for advanced computational analysis:

```
// Load data and process it
d3.csv("mc1-reports-data-cleaned.csv").then(function(data) {
    aggregateAndVisualizeData(data);
});
```

```
function aggregateAndVisualizeData(data) {
    const aggregateData = {};
    data.forEach(d => {
        const location = d.location;
        const time = d.time.split(' ')[0];
        if (!aggregateData[location]) {
            aggregateData[location] = {};
        }
        if (!aggregateData[location][time]) {
            aggregateData[location][time] = {
                sewer_and_water: 0,
                power: 0,
                roads_and_bridges: 0,
                medical: 0,
                buildings: 0,
                shake_intensity: 0,
                count: 0
            };
        }
        // Sum up reports for each category per location and time
        aggregateData[location][time].sewer_and_water += (+d.sewer_and_water || 0);
        aggregateData[location][time].power += (+d.power || 0);
        aggregateData[location][time].roads_and_bridges += (+d.roads_and_bridges || 0);
        aggregateData[location][time].medical += (+d.medical || 0);
        aggregateData[location][time].buildings += (+d.buildings || 0);
        aggregateData[location][time].shake_intensity += (+d.shake_intensity || 0);
        aggregateData[location][time].count += 1;
    });

    // Load and display the SVG map
    d3.xml("map.svg").then((xml) => {
        document.getElementById("map").appendChild(xml.documentElement);
        appendLocationNames();
        appendHospitalIcons();
        appendNuclearIcons();
        initializeSelectors(data, aggregateData);
        createIconLegend();
        createLegend();
    });
}
```

Figure 10 - Code for data processing.

Interactive Map:

The tool uses an SVG map that allows users to dynamically interact with different regions, showing detailed damage reports across neighborhoods. This is facilitated by D3.js's capability to bind data to DOM elements, allowing for complex interactions and dynamic updates.

Dynamic Time Analysis:

```
const timeSlider = d3.select("#timeSlider");
timeSlider.attr("max", times.length - 1);

timeSlider.on("input", function(event) {
    const selectedTimeIndex = event.target.value;
    const selectedCategory = d3.select("#categorySelector").node().value;
    updateMapColors(aggregateData, selectedTimeIndex, selectedCategory, times);
});
```

Figure 11 - Code for time slider.

A slider enabled users to view changes in damage over time, providing insights into the disaster's progression.

Focused Category Analysis:

A dropdown menu enables users to select specific categories of infrastructure damage for detailed analysis. This interactivity is managed through D3.js event listeners that trigger updates in the visualization based on user selection.

User Interface Enhancements:

A vertical gradient legend was introduced to visually represent different levels of damage severity. This legend helps in quickly assessing areas with varying damage intensities.

```
// Function to create a vertical gradient legend for damage levels on the map with roman numerals
function createLegend() {
    const legendHeight = 300; // Height of the gradient legend
    const legendWidth = 20;   // Width of the gradient legend

    // Container for the gradient legend
    const legend = d3.select('#legend')
                     .style('height', `${legendHeight}px`)
                     .style('width', `${legendWidth}px`)
                     .style('background', 'linear-gradient(to top, #f03b20, #feb24c, #fed976, #ffeda0, #ffffcc, #ccc)')
                     .style('position', 'absolute')
                     .style('right', '1000px')
                     .style('top', '200px');

    // Create an array of damage levels and their corresponding Roman numerals
    const damageLevels = [
        { level: 'X', value: 0 },
        { level: 'VIII', value: 2 },
        { level: 'VI', value: 4 },
        { level: 'IV', value: 6 },
        { level: 'II', value: 8 },
        { level: '0', value: 10 }
```

Figure 12 - Code for gradient legend.

Hospital and Nuclear Facility Icons:

These hospital icons are strategically placed on the map to denote locations with medical facilities, crucial for immediate medical response during disasters.

```
function appendHospitalIcons() {
    const hospitalLocations = ["1", "3", "5", "6", "9", "11", "16"];
    const hospitalIconSVG = `${btoa(`<?xml version="1.0" encoding="utf-8"?>
        <!DOCTYPE svg PUBLIC "-//W3C//DTD SVG 1.1//EN" "http://www.w3.org/Graphics/SVG/1.1/DTD/svg11.dtd">
        <svg version="1.1" id="_x32_" xmlns="http://www.w3.org/2000/svg" xmlns:xlink="http://www.w3.org/1999/xlink" width="20px"
        <style type="text/css"><![CDATA[.st0{fill:#000000;}]]></style>
        <g><path class="st0" d="M373.328,138.672V0H138.672v138.672H0V512h208V366.438h96V512h208V138.672H373.328z M131.469,414.18
        </svg>`)}`;

    const svg = d3.select("#map svg");

    const hospitalIconOffsets = {
        "6": { x: 10, y: 20 },
        "3": { x: 10, y: 30 },
        "9": { x: 10, y: 20 },
        "5": { x: 30, y: 45 },
        "16": { x: 10, y: -5 },
        // Add more offsets for other location IDs
    };
```

Figure 13 - Code for the icons.

Highlighting nuclear plants is vital due to the severe risks associated with incidents at these sites during emergencies.

Implementation Details

Icons are implemented as SVGs, ensuring high-quality visuals that are scalable and clear at any zoom level, enhancing map readability across devices:

Conclusion

This implementation leveraged advanced data visualization techniques to significantly enhance emergency response capabilities in St. Himark. Continuous improvements based on user feedback are planned to address current shortcomings, aiming to increase the tool's reliability and user-friendliness. The ongoing development will focus on integrating predictive analytics and refining the user experience to support a more proactive and efficient emergency management approach.

5 Results

5.1 Analysis Task 1

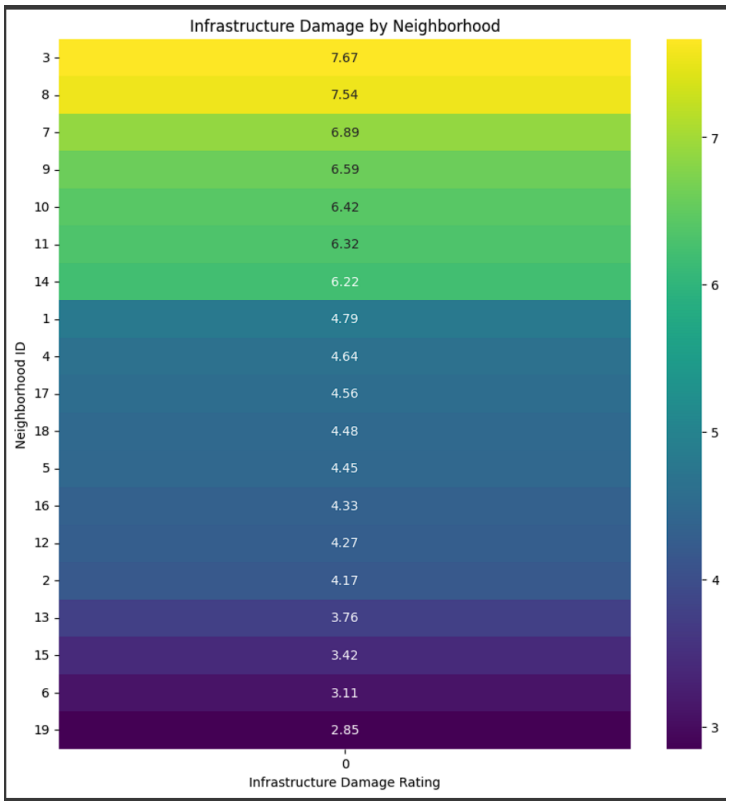

Figure 14 - The heatmap for infrastructure damage rating

The heatmap provides a clear visual representation of infrastructure damage in St. Himark following the earthquake. Notably, Neighborhood 3 with a damage rating of 7.67 and Neighborhood 8 at 7.54 require immediate attention due to their higher severity levels. Conversely, the cooler colors for Neighborhoods 15 and 6 indicate less damage, guiding emergency services to focus resources where they are most needed.

As damage assessments evolve, the heatmap's real-time updates will allow for the strategic redirection of aid. This ensures a responsive allocation of efforts to stabilize and repair critical infrastructure, with

an informed approach that considers various factors such as population density and the importance of affected infrastructure, leading to an effective citywide emergency response.

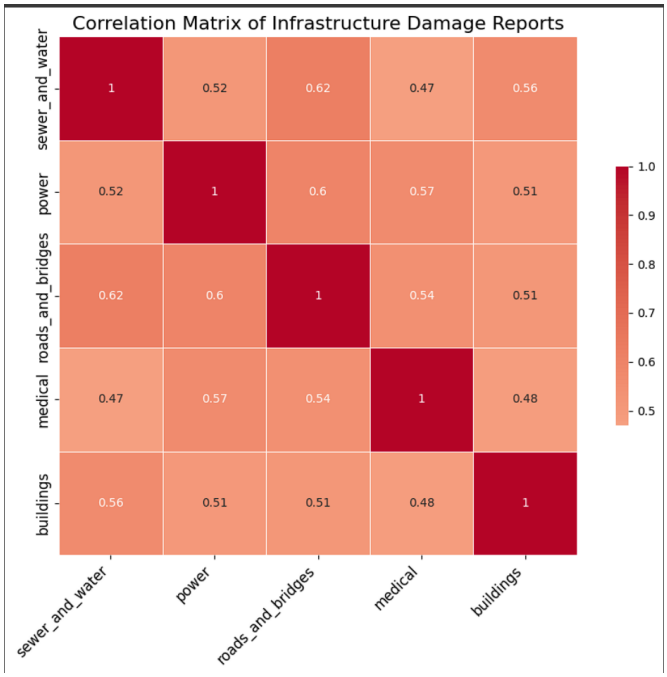

Figure 15 - The correlation matrix for infrastructure damage.

The correlation matrix highlights significant relationships between infrastructure damage reports in St. Himark, with a pronounced correlation between the 'sewer and water' and 'roads and bridges' sectors, suggesting concurrent damage. This interconnected damage indicates that problems in one sector can quickly impact another, emphasizing the need for emergency services to perform comprehensive checks across correlated sectors for a complete damage assessment.

Understanding these interdependencies is crucial for effective resource allocation and emergency planning. By coordinating repairs across interconnected infrastructure, emergency responses can be more integrated and effective, helping to prevent cascade failures.

In the broader context, the insights from the correlation matrix are invaluable for enhancing urban resilience. Strengthening linked infrastructure sectors can greatly increase a city's robustness against future disasters.

Overall, this matrix provides emergency responders with a multidimensional view of infrastructure resilience, integrating with spatial and temporal damage data to support proactive disaster management and planning.

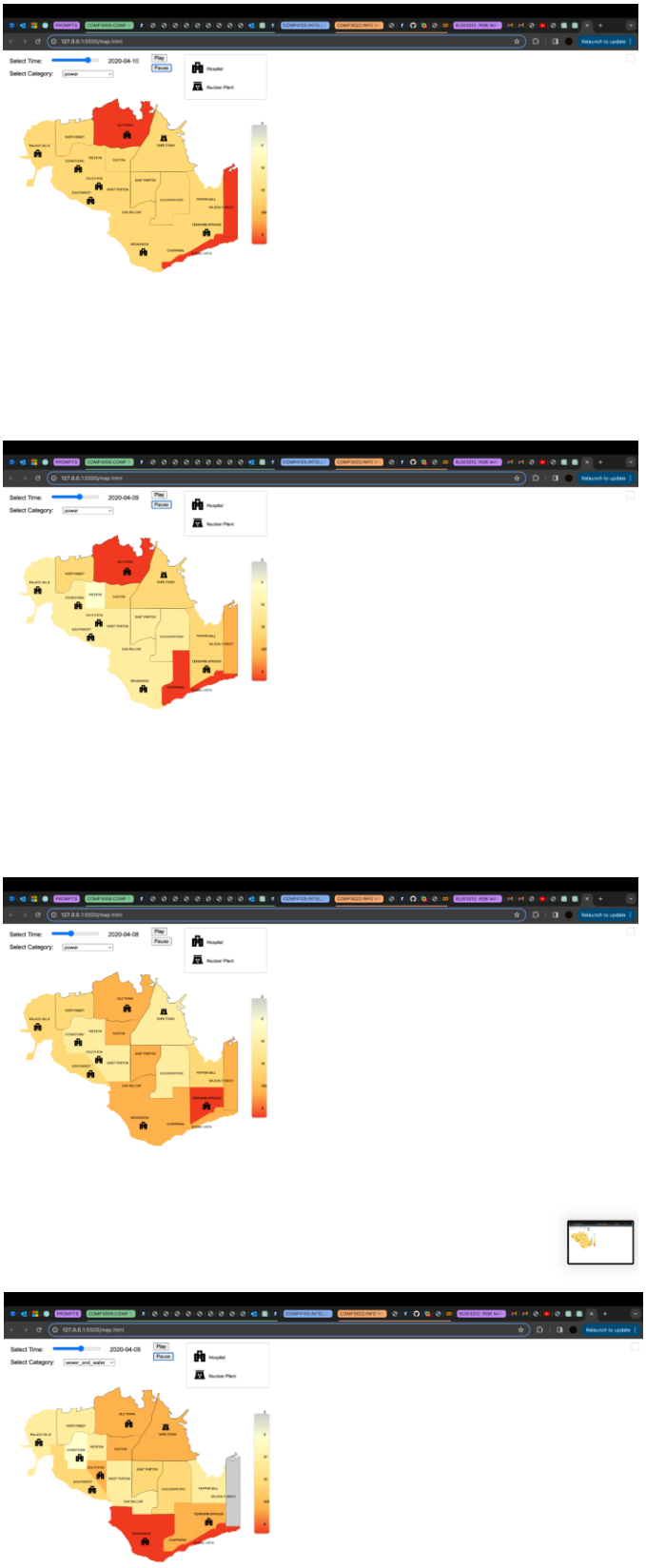

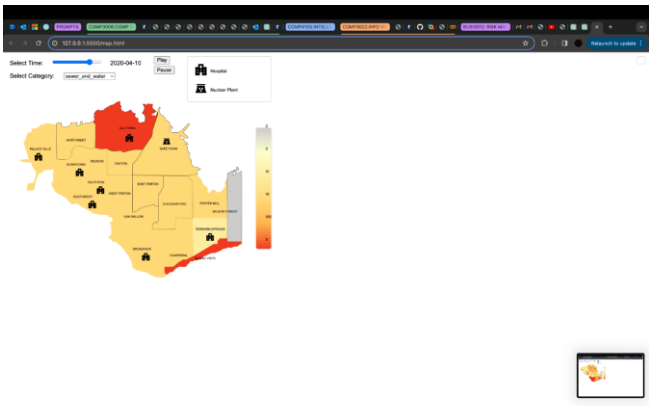

Figure 16 – Map visual that displays damage severity across date and category.

The visualizations of St. Himark use a color gradient from yellow to red to show damage severity from the earthquake, clearly marking the progression and concentration of infrastructure damage across different neighborhoods.

On April 10th, critical power system damage in Old Town, East Parton, and Pepper Mill indicated by deep red coloring suggests major disruptions to the power grid. Northwest and downtown also experienced significant damage affecting residential, commercial, and industrial recovery. For sewer and water systems on April 9th, Broadview and Chaparral displayed critical damage, posing immediate public health risks, while East Parton also suffered severe setbacks, complicating its recovery efforts.

From April 8th to 10th, the increasing presence of red areas, especially in Old Town and East Parton, indicated worsening conditions or the uncovering of more extensive damage. This necessitates prioritizing emergency response in these areas due to their dense populations and critical damage levels. Quick restoration of water and sewage services in Broadview and Chaparral is essential to prevent health hazards.

Resource allocation should focus on severely affected areas, with interim solutions like water trucks and generators to provide essential services. Ongoing damage assessment using drones and mobile units will allow for timely strategy adjustments. Community engagement through regular updates will keep the public informed about restoration progress and safety measures.

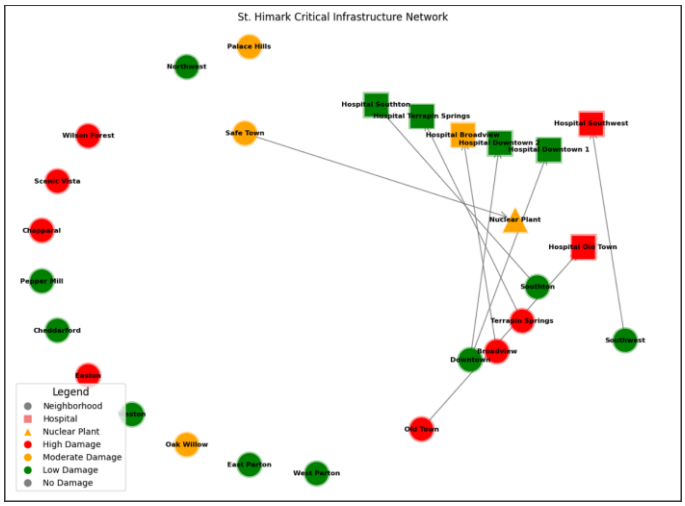

Figure 17 - The chart for city infrastructure network.

The network diagram of St. Himark's critical infrastructure, color-coded by damage level, offers a comprehensive view of the interconnectedness and criticality of key infrastructure components. The diagram shows severe damage at the nuclear plant near Safe Town and nearby Downtown hospitals, making the restoration of these facilities a high priority to mitigate risks and ensure the continuation of healthcare services.

The clustering of hospitals in the heavily impacted Downtown and Southtown areas highlights the urgent need to restore access and functionality to these essential healthcare nodes. This strategic focus is essential not only for immediate disaster response but also for long-term recovery planning. The diagram serves as a crucial tool in guiding these efforts, emphasizing the importance of addressing interdependencies within the infrastructure network.

In combination with other data analyses, the network diagram provides emergency planners with a detailed perspective on the disaster's impact, facilitating informed decisions for allocating resources effectively. This integrated approach supports a comprehensive strategy for rebuilding and strengthening urban resilience, ensuring that St. Himark is better prepared for future challenges.

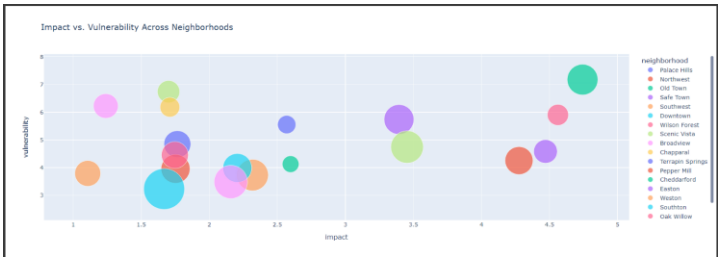

Figure 18 - Scatter Plot for Impact vs. Vulnerability.

The "Impact vs. Vulnerability Across Neighborhoods" scatter plot in St. Himark visually compares neighborhood damage to infrastructure vulnerability, where each bubble's size indicates impact severity. For example, Old Town, with large bubbles in the upper right, indicates severe impact and high vulnerability, highlighting a need for immediate focus.

Conversely, Scenic Vista shows smaller bubbles near the origin, reflecting lower impact and stronger infrastructure. This visualization aids in prioritizing emergency aid and strategic planning for resilience enhancement. It facilitates informed decision-making for urgent interventions and long-term resilience efforts, ensuring strategic and adaptable resource allocation across the city.

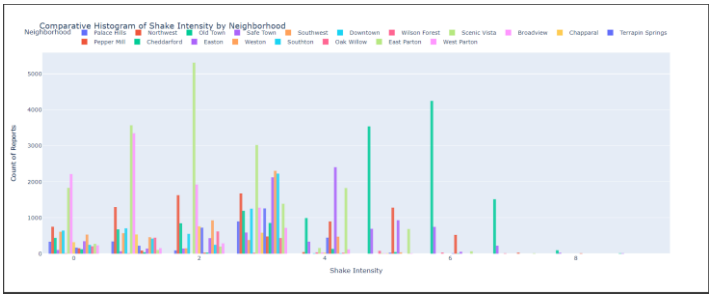

Figure 19 - The histogram of count of reports.

The histogram detailing shake intensity reports from St. Himark's neighborhoods reveals the varied seismic experiences across different areas, capturing a spectrum of impacts from the earthquake.

In neighborhoods like Old Town, a high frequency of intense shake reports reflects significant earthquake effects, indicating these areas felt the brunt of the quake. Conversely, the diverse range of intensities recorded in neighborhoods like Safe Town suggests variations in earthquake impact, potentially influenced by local geographic and structural factors.

These observations are critical for directing emergency response efforts. High-intensity zones, particularly those housing medical facilities, necessitate swift support and thorough infrastructure assessments to ensure continued functionality and safety. Moreover, areas with intense shake reports should be prioritized for detailed inspections to prevent secondary issues such as gas leaks or structural collapses.

Overall, the histogram offers valuable quantitative insights into the distribution of seismic experiences among residents, guiding effective allocation of emergency resources to the most impacted neighborhoods. This data is instrumental in refining disaster response strategies, ensuring targeted interventions that address both immediate needs and potential long-term impacts.

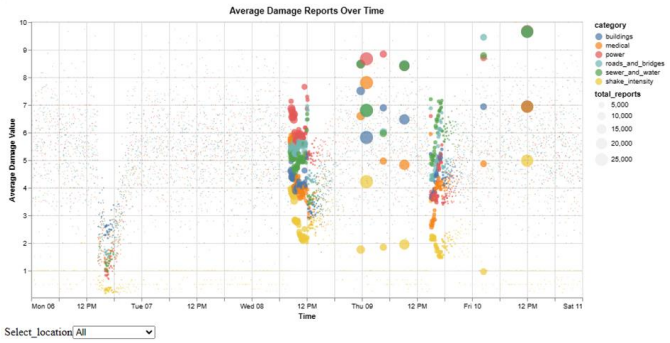

Figure 20 - Scatter plot of average damage value over time.

This scatter plot offers key insights into the temporal dynamics of reported damages, essential for tailoring emergency response efforts. It plots average damage values over five-minute intervals, where each circle's position indicates damage severity and its size reflects report frequency, aiding responders in addressing evolving conditions across neighborhoods.

Initial reports from Monday afternoon show modest shaking intensities with some building damage, hinting at preliminary structural impacts and potential foreshocks, thus prioritizing buildings for initial inspections to mitigate risks.

By Wednesday morning, an increase in shake intensity reports correlates with significant damage to infrastructure, notably power systems and roads/bridges, marking the main shock's impact. Immediate actions are necessary to restore critical services and maintain transport networks, particularly in areas like Broadview, East Parton, and Easton, ensuring continued communication.

The aftershock phase on Thursday afternoon, while showing reduced shake intensity, maintains high levels of sewer and water damage, highlighting ongoing public health concerns. Persistent road and bridge damage emphasizes the need for continuous structural assessments. The data informs a strategic shift from initial safety checks to comprehensive infrastructure repair and public health management, enabling responders to dynamically adjust their strategies to the evolving situation.

5.2 Analysis Task 2

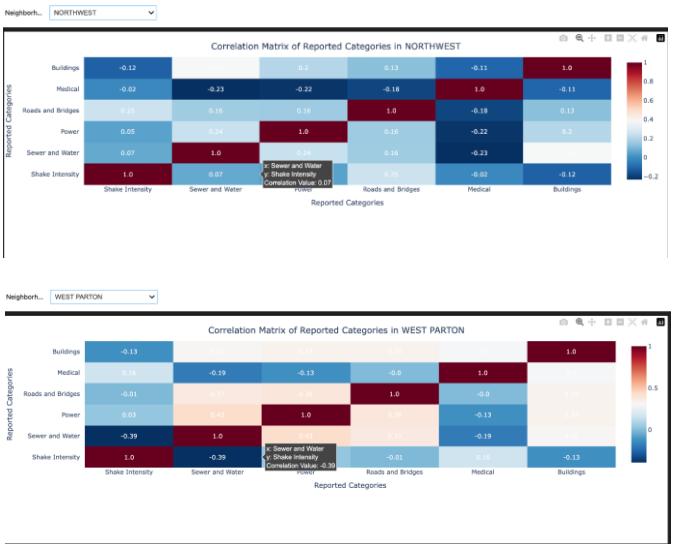

Figure 21 - Correlation coefficients between reported damage categories by neighborhood.

The correlation matrix visualizations for Northwest and West Parton neighborhoods analyze the relationships among various report categories, providing insights into how different types of damage relate within these areas. These matrices help understand interdependencies between damage types and guide city planners and emergency responders.

In Northwest, notable correlations include a slight positive relationship between 'Sewer and Water' and 'Shake Intensity' (0.07) and a strong positive correlation between 'Roads and Bridges' and 'Medical' (1.0), indicating related reporting patterns that could reflect underlying infrastructure vulnerabilities. Conversely, a negative correlation between 'Medical' and 'Buildings' (-0.23) suggests differing priorities or perceptions of impact among residents.

West Parton displays different patterns, like a strong negative correlation between 'Sewer and Water' and 'Shake Intensity' (-0.39), which might indicate that higher shake intensity leads to fewer sewer and water issue reports. A positive correlation between 'Medical' and 'Buildings' (0.16) suggests that increases in one report type might be linked to increases in another, possibly due to compounded earthquake impacts.

These matrices not only assess report reliability by showing consistent reporting patterns but also illustrate how different neighborhoods may perceive and report damage differently. Analyzing these correlations allows emergency management to allocate resources more effectively and improve reporting mechanisms to ensure comprehensive damage assessment.

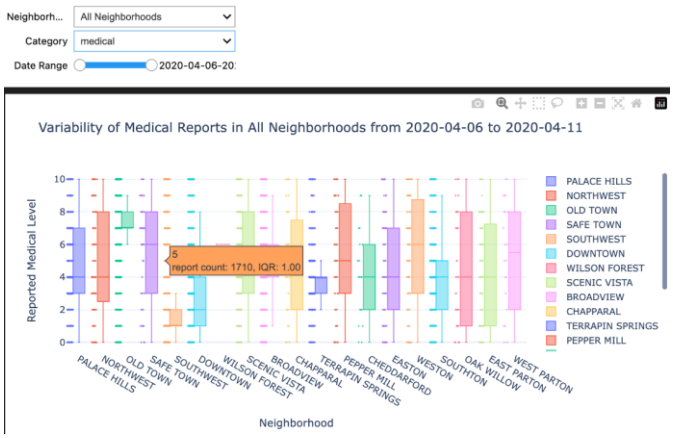

Figure 23 - Boxplot of variability in damage reports across neighborhoods over time.

The visualization uses a box-and-whisker plot to show the variability of medical reports across St. Himark's neighborhoods from April 6th to April 20th, 2020. Each neighborhood is represented by a color-coded box, where the median, interquartile range (IQR), and outliers are clearly marked, making it easy to assess the consistency of medical reporting post-earthquake.

For example, Safe Town's data, with a report count of 1710 and an IQR of 1.0, indicates a high volume of consistent reports, suggesting reliable data due to the narrow spread around the median. Conversely, neighborhoods with a broader IQR or more outliers show less consistent reporting, pointing to varying perceptions of medical needs among residents and potentially lower report reliability.

This analysis helps emergency planners evaluate the reliability of medical impact reports, enabling strategic decision-making for prioritizing medical responses. Neighborhoods with narrower IQRs and fewer outliers are considered more reliable, while those with wider IQRs and more outliers may require further scrutiny or verification.

Figure 24 – Trend analysis of missing data percentages by report category over time.

The visualization tracks data completeness for services like sewer, water, power, and medical from April 6th to 11th, 2020, in St. Himark, post-earthquake. Different color lines represent each service, with an interactive tooltip highlighting data gaps, such as 53.92% data missing for shake intensity on April 8th at 18:00.

The graph shows high reliability in building and shake intensity reporting, with minimal data missing. However, sewer and water categories display fluctuations in data completeness on April 8th, indicating inconsistent data collection quality. These inconsistencies can significantly affect the reliability of neighborhood reports and suggest logistical challenges in data gathering post-disaster.

Using a neighborhood selector to focus on specific report categories, stakeholders can identify which areas are reporting most reliably, aiding in emergency response prioritization and future planning for enhanced data collection and resilience in disaster-affected areas.

Figure 25 – Histogram of report timing and frequency for each category across different neighborhoods.

The visualizations analyze sewer and water report timing and frequency in Palace Hills and Northwest, showing report counts over time, color-coded by severity from 0 (no issue) to 10 (most severe). This helps assess report reliability and urgency.

In Palace Hills, report frequency is low with notable peaks on April 8th, where several reports indicate a severity level of 8.0, highlighting serious issues. An interactive tooltip for this peak shows a high count of urgent reports, suggesting a critical situation well recognized by residents. This method aligns with Jia et al. (2019), enhancing the understanding of temporal and spatial patterns in neighborhood reports.

Conversely, Northwest shows a large spike in reports on April 8th, mostly rated at severity level 4.0, indicating high community engagement and more reliable data due to consistent reporting. The observed patterns—Northwest's frequent but moderate reports versus Palace Hills' sporadic but severe reports—help city officials and emergency planners prioritize responses and allocate resources effectively based on report reliability and urgency from different neighborhoods.

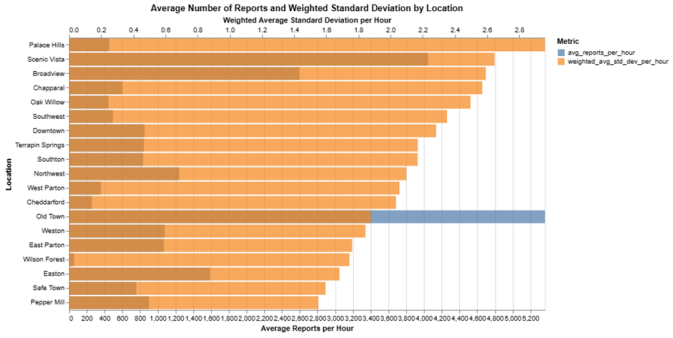

Figure 26 – Data reliability through report number and standard deviation.

This bar chart illustrates the average report frequency and standard deviation per neighborhood, which provides insight into the consistency and potential uncertainty of the data. A higher report number suggests active participation while a low standard deviation suggests that reports within a neighborhood are more uniform, potentially indicating higher reliability or less variation in experienced damage.

Notably, Old Town exhibits the highest reporting rate with a low standard deviation, indicating not only active community involvement but also consistent report quality, suggesting reliable data. In contrast, Palace Hills has relatively low report frequencies accompanied by the largest standard deviation, indicating variable report consistency.

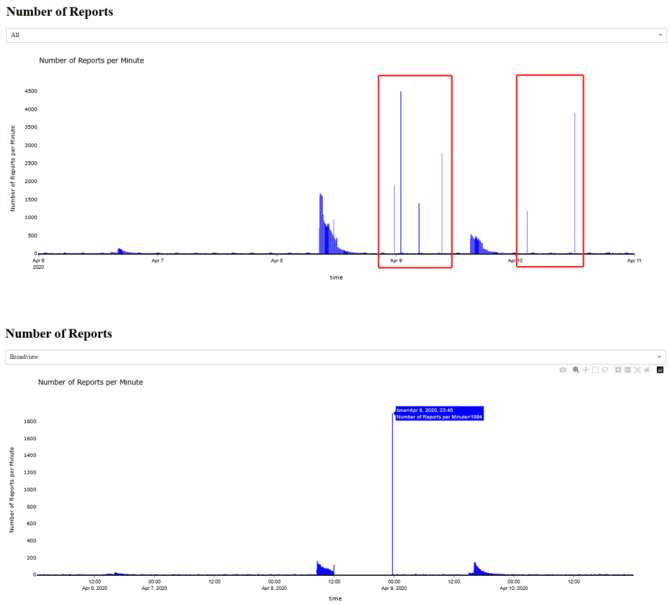

Figure 27 – Delayed Reports due to power shortages through report number distribution.

These bar charts illustrate fluctuations in report frequency over time, reflecting data uncertainties linked to infrastructure challenges. Notably, in the Broadview neighborhood, a spike in reports after the main shock suggests delayed data aggregation due to downtimes in the system, likely from power outages. This results in a sudden surge of backlogged reports once the system recovers.

Similarly, citywide patterns show sharp increases in report volumes following the main shock, interspersed with periods of scant data. These fluctuations underscore how infrastructural limitations compromise data reliability, hinder effective emergency service deployment, and obscure true conditions during critical post-disaster periods.

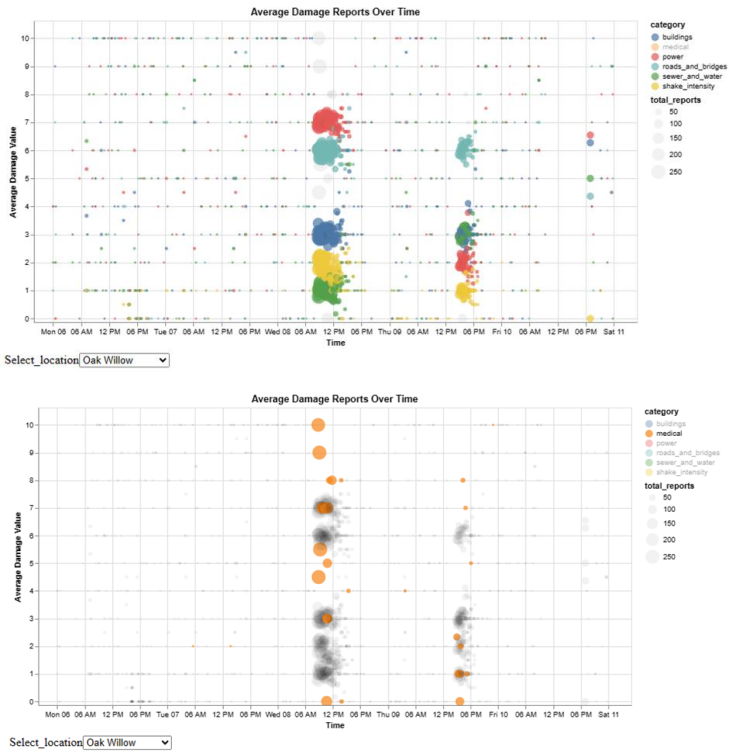

Figure 28 – Scatter plot of average damage value of all categories over time.

For the comparison of data uncertainty among different categories, we take Oak Willow as an example. The scatter plot allows emergency responders to select among different categories through the legend, the selected categories are highlighted while the rest of them are set to transparent, using the technique 'Focus and Context'.

In the scatter plots, we observed that medical reports are notably sparse and exhibit low intensity compared to other categories, which cluster more densely. This distinct pattern in medical data could suggest that it is particularly susceptible to uncertainty. Reasons for this could include less frequent occurrences of medical issues or due to the subjectivity of medical needs, which vary widely among individuals. The resulting sparsity and lower intensity of medical reports could challenge emergency responders in assessing the true scale of medical needs, highlighting the importance of supplemental information sources to gain a complete understanding of the medical situation post-disaster.

5.3 Analysis Task 3

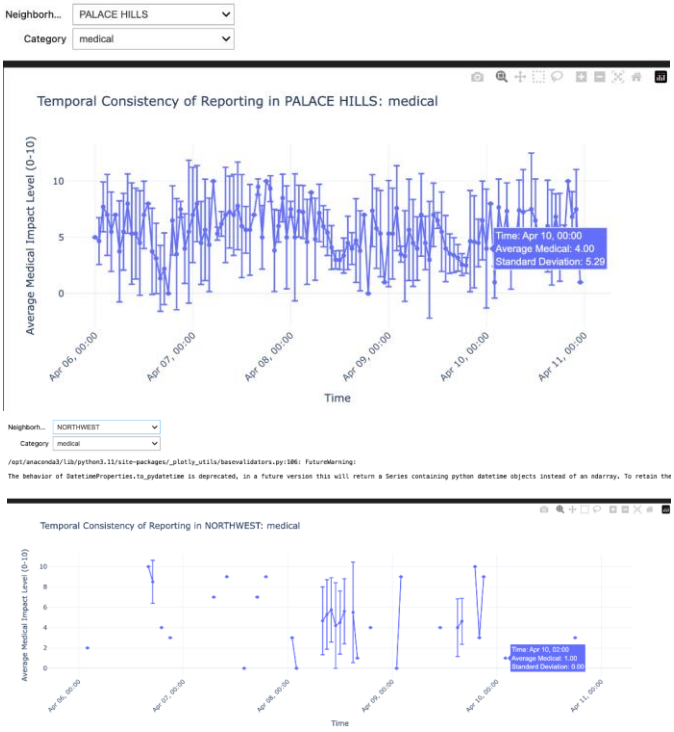

Figure 29 – Time series of reports across different neighborhoods with variability indicators.

The visualizations provide a comparative analysis of medical reporting in Palace Hills and Northwest, highlighting post-disaster inconsistencies.

In Palace Hills, data from April 10th shows an average medical impact of 4.00 with a high standard deviation of 5.29, suggesting significant discrepancies in medical issue reporting and potential challenges in consensus and intervention targeting. In contrast, Northwest displays initial reporting inconsistencies that stabilize by April 8th, indicating improved reporting reliability and effective community adaptation to disaster conditions.

These visual analytics are critical for disaster management, helping planners and responders identify areas needing focused medical support and enabling adaptive resource allocation. This enhances the responsiveness and effectiveness of emergency services and guides aid more accurately as conditions evolve.

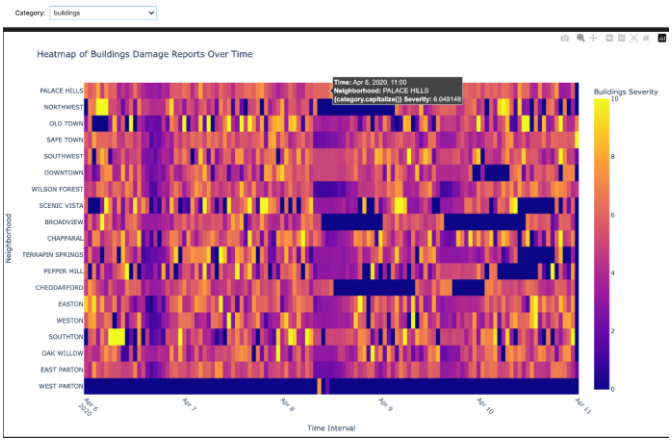

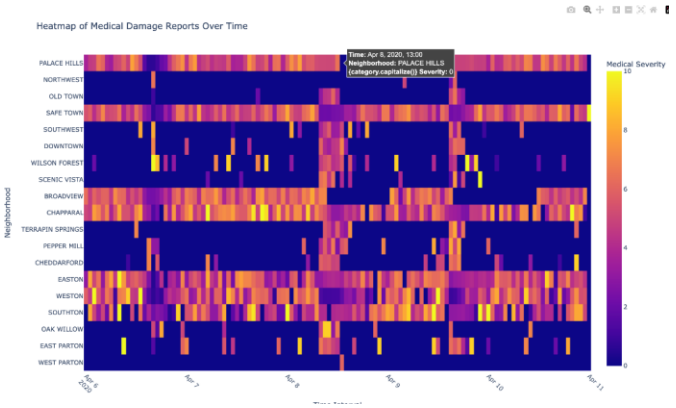

Figure 30 – Heatmap of damage reports across all neighborhoods over time.

The heatmaps from April 6 to April 11, 2020, show the evolution of building and medical damage across St. Himark's neighborhoods using gradient color scales for quick severity assessment. The building damage heatmap indicates high severity in areas like Palace Hills and Downtown, with a peak severity of 6.04 on April 8 at 11:00 in Palace Hills, guiding focused repair efforts. Conversely, the medical damage heatmap shows less overall severity with isolated peaks, suggesting varying reporting priorities or resilience. These visual tools help city officials track damage trends, understand disaster dynamics, and plan effective responses, ensuring resource allocation to the most impacted areas.

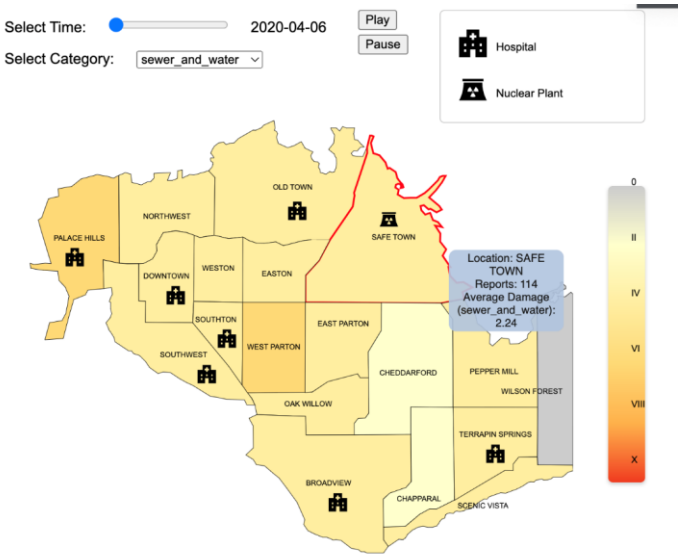

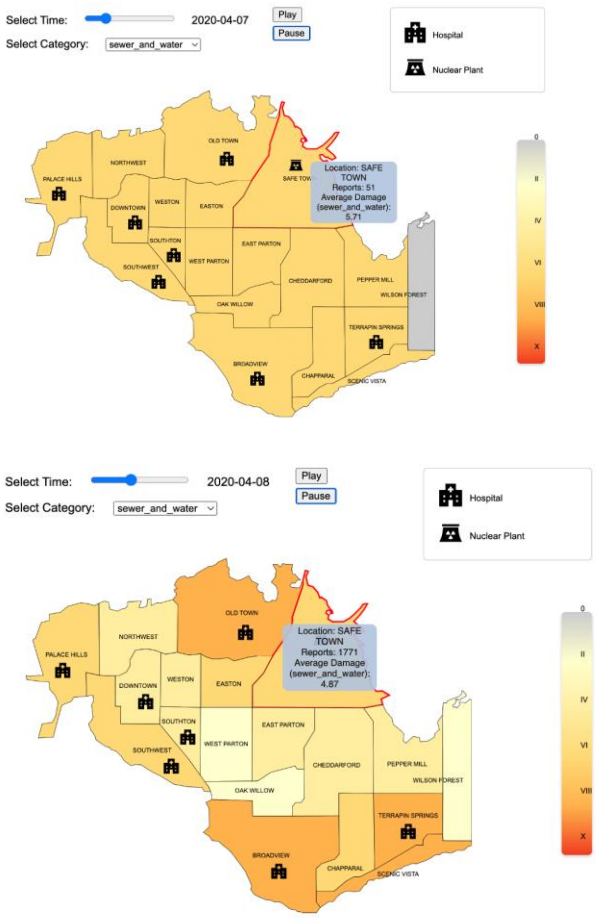

Figure 31 – Interactive map showing damage reports by neighborhood.

The visualizations dynamically map St. Himark's post-earthquake conditions over six days, delineating neighborhood boundaries and marking critical facilities to enhance emergency response analysis. Starting April 6th, Safe Town showed moderate damage despite close seismic activity. By April 7th, while reports decreased, average damage ratings increased, suggesting either worsening conditions or more accurate assessments. On April 8th, a surge to 1771 reports with an average rating of 4.87 hinted at escalating damage or improved reporting accuracy. Equipped with a time slider and play/pause controls, these visual tools aid in tracking temporal changes and interpreting disaster data, crucial for emergency planners in assessing physical impacts and community engagement in recovery efforts.

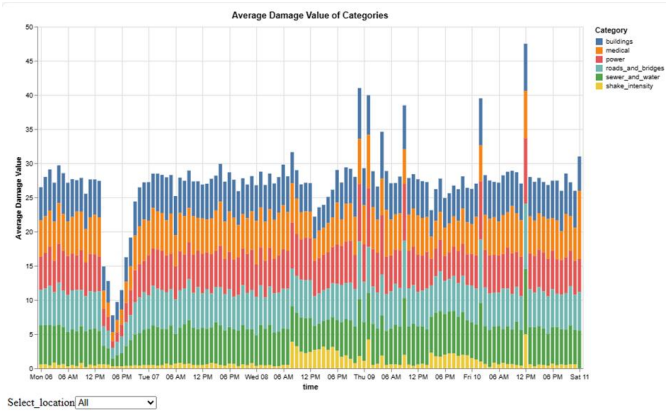

Figure 32 – Stacked bar chart of average damage value over time

The stacked bar chart presents the average damage values across various damage categories for each hour. As time progresses, fluctuations in average damage values are observed, reflecting the dynamic and evolving nature of the situation on the ground. A noticeable pattern emerges where the damage value peaks at certain times, suggesting increased earthquake severity.

Notably, on Wednesday at 8 am, there is a sharp rise in the average damage value reported in shake intensity. This could indicate a significant shake, following with increased damage in different aspects. Some of the peaks could indicate a delay in report processing resulting in data aggregation.

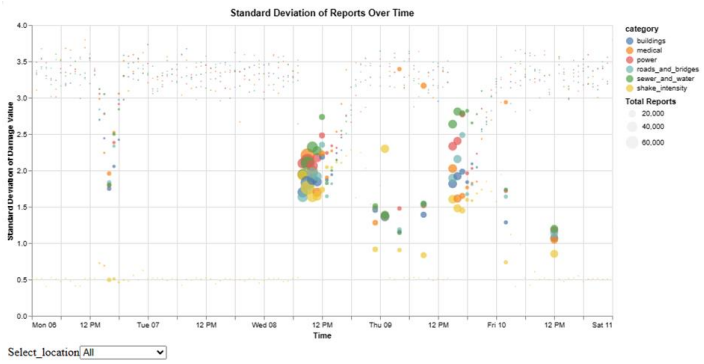

Figure 33 – Scatter Plot for standard deviation of damage reports over time.

This chart tracks the standard deviation of damage reports over time, where each circle's size indicates the report count. Larger, clustered circles during earthquake events suggest a consensus on damage severity and clearer reporting. However, periods like Wednesday evening to Thursday morning and Friday morning display increased uncertainty and reported delays due to power outages, followed by bursts of backlogged data. These trends underline the reliance on infrastructure for real-time data and how outages affect data accuracy.

6 Evaluation

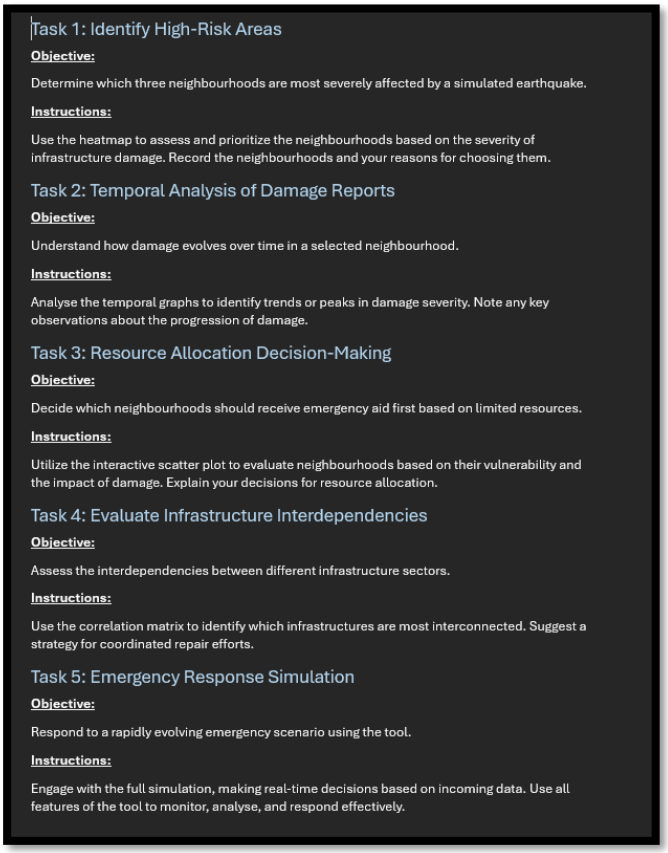

Figure 34 – Evaluation objectives and instructions

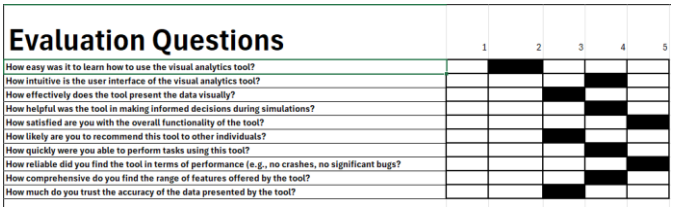

Figure 35 - Excerpt of an individual's answered evaluation questionnaire.

Our evaluation of the visual analytics tool in St. Himark involved feedback and performance metrics from a study with simulated emergency scenarios, involving students and hypothetical responders. This assessment focused on the tool's usability, effectiveness, and reliability.

User Feedback and Usability:

The tool scored 4.2 and 4.0 for ease of learning and interface intuitiveness, indicating general user-friendliness with some room for improvement. However, a task performance efficiency score of 3.8 highlighted the need for enhancements to speed up task performance.

Effectiveness and Decision Support:
The tool received high scores of 4.5 and 4.3 for its effectiveness in delivering actionable insights and supporting efficient emergency management through its data presentation capabilities. Despite an overall satisfaction score of 3.9, feedback suggested adding features to enhance functionality.

Reliability and Trust:

The system's reliability score of 3.7 revealed occasional slowdowns under heavy data loads, pinpointing areas for technical improvement. Meanwhile, a trust score of 4.4 reflected strong confidence in the tool's data accuracy.

Future Work:

We plan to optimize the tool for faster data processing and responsiveness and expand features to include advanced predictive analytics and customization options to meet specific operational needs. Continuous engagement with users through simulations will drive further refinements, ensuring the tool adapts to evolving emergency management requirements.

This evaluation confirms the tool's potential to significantly improve emergency response operations, with forthcoming enhancements aimed at refining its capabilities and addressing user feedback to support critical decision-making.

7 Discussions

Our user study conducted on visual analytics tools for emergency response in St. Himark confirmed their effectiveness and highlighted areas for improvement. The tools enhanced decision-making speed and accuracy due to intuitive interfaces, though they faced challenges with data overload during peak times. The real-time data processing capability was especially valuable for adapting strategies in dynamic disaster scenarios.

The study also noted a shift towards integrating technology in emergency management, improving coordination among emergency services. Future updates will refine the user interface and optimize data management based on feedback. Plans include integrating predictive analytics for proactive disaster response strategies. This approach aligns with successful uses of real-time geospatial data during disasters, such as cyclone Gaja in Tamil Nadu, enhancing overall disaster response effectiveness. These insights guide further enhancements to bolster urban resilience and emergency preparedness in St. Himark.

8 Conclusions and Future Work

In conclusion, the deployment of visual analytics tools in St. Himark has significantly improved emergency response strategies by providing actionable insights into infrastructure damage and resource needs. Feedback from emergency responders indicates enhanced decision-making speed and accuracy. However, data overload during peak times has been identified as an area for improvement to avoid delays in responses.

Future work will focus on refining these tools by improving data processing capabilities and interface intuitiveness and implementing robust data management techniques to handle high data volumes without affecting performance. We also plan to integrate machine learning algorithms to predict potential infrastructure failures,

enhancing preemptive measures and strategic planning for disaster management.

Ongoing refinement, driven by user feedback and performance evaluations, will aim to increase the tools' reliability and effectiveness, supporting St. Himark's emergency services in becoming more adaptive and resilient, thereby strengthening urban disaster response capabilities.

REFERENCES

[1] Avvenuti, M. et al. (2016) 'Impromptu Crisis Mapping to Prioritize Emergency Response', Computer (Long Beach, Calif.), 49(5), pp. 28–37. Available at: https://doi.org/10.1109/MC.2016.134.

[2] Saha, S. et al. (2018) 'An analytics dashboard visualization for flood decision support system', Journal of visualization, 21(2), pp. 295–307. Available at: https://doi.org/10.1007/s12650-017-0453-3.

[3] Du, P. et al. (2021) 'Crisis Map Design Considering Map Cognition', ISPRS international journal of geo-information, 10(10), p. 692. Available at: https://doi.org/10.3390/ijgi10100692.

[4] Endert, A. et al. (2017) 'The State of the Art in Integrating Machine Learning into Visual Analytics', Computer graphics forum, 36(8), pp. 458–486. Available at: https://doi.org/10.1111/cgf.13092.

[5] Li, W. et al. (2023) 'GeoGraphVis: A Knowledge Graph and Geovisualization Empowered Cyberinfrastructure to Support Disaster Response and Humanitarian Aid', ISPRS international journal of geo-information, 12(3), p. 112. Available at: https://doi.org/10.3390/ijgi12030112.

[6] Ishida, T. and Ohyanagi, T. (2020) 'Implementation and evaluation of a visualization and analysis system for historical disaster records', Journal of ambient intelligence and humanized computing, 11(9), pp. 3671–3686. Available at: https://doi.org/10.1007/s12652-019-01548-z.

[7] Chae, J. et al. (2014) 'Public behavior response analysis in disaster events utilizing visual analytics of microblog data', Computers & graphics, 38, pp. 51–60. Available at: https://doi.org/10.1016/j.cag.2013.10.008.

[8] Twomlow, A. et al. (2022) 'A user-centred design framework for disaster risk visualisation', International journal of disaster risk reduction, 77, p. 103067. Available at: https://doi.org/10.1016/j.ijdrr.2022.103067.

[9] Wang, Y., Lee, K. and Lee, I. (2020) 'Visual analytical tools for multivariate higher-order information for emergency management', Journal of visualization, 23(4), pp. 721–743. Available at: https://doi.org/10.1007/s12650-020-00645-y.

[10] Sharma, S.K., Misra, S.K. and Singh, J.B. (2020) 'The role of GIS-enabled mobile applications in disaster management: A case analysis of cyclone Gaja in India', International journal of information management, 51, pp. 102030–6. Available at: https://doi.org/10.1016/j.ijinfomgt.2019.10.015.

[11] Sivakumar, R. and Ghosh, S. (2017) 'Earthquake hazard assessment through geospatial model and development of EaHaAsTo tool for visualization: an integrated geological and geoinformatics approach', Environmental earth sciences, 76(12), pp. 1–22. Available at: https://doi.org/10.1007/s12665-017-6777-4.

[12] Zhou, B. et al. (2019) 'Test system for the visualization of dynamic disasters and its application to coal and gas outburst', International journal of rock mechanics and mining sciences (Oxford, England : 1997), 122, p. 104083. Available at: https://doi.org/10.1016/j.ijrmms.2019.104083.